

UNIVERSITY of CALIFORNIA
SANTA CRUZ

**DYNAMIC STUDIES OF PUNCH THROUGH PROTECTION OF
SILICON STRIP DETECTORS WITH LASER-BASED CHARGE
INJECTION SYSTEM**

A thesis submitted in partial satisfaction of the
requirements for the degree of

BACHELOR OF SCIENCE

in

ASTROPHYSICS

by

Mykhaylo Shumko

15 June 2014

The thesis of Mykhaylo Shumko is approved by:

Dr. Vitaliy Fadeyev
Advisor

Professor David P. Belanger
Theses Coordinator

Professor Michael Dine
Chair, Department of Physics

Copyright © by

Mykhaylo Shumko

2014

Abstract

Dynamic studies of punch through protection of silicon strip detectors with
laser-based charge injection system

by

Mykhaylo Shumko

Large implant voltages caused by beam losses have the potential to damage A Toroidal Large Hadron Collider Apparatus (ATLAS) silicon strip sensors. These sensors are used in the ATLAS detector located in the Large Hadron Collider (LHC). The Punch Through Protection (PTP) is an N-P-N doped structure on the silicon sensors which protects the sensor in the event of a large implant voltage. Charge was injected into the biased sensor via an IR laser. We probed the voltage at either end of the implant. When the ATLAS12 BZ3C P6 sensor was biased to a voltage below 300 V, the PTP structure near the bias resistor had a varying resistance which ranged from $18 \text{ k}\Omega$ at 50 V bias voltage to $9 \text{ k}\Omega$ at 250 V bias voltage. The PTP structure farthest from the bias resistor on the ATLAS12 BZ3C P16 sensor had a constant resistance of roughly $200 \text{ k}\Omega$ that did not significantly change with increasing bias voltage. The sensors that were biased to 300 V and subjected to laser injection all showed a large increase in leakage current after the testing. After the PTP resistance measurements were made, it was possible to determine the most effective PTP geometry. A more effective PTP structure is characterized by a lower resistance and will greatly minimize the damage from a beam loss at the LHC.

Contents

List of Figures	v
List of Tables	vii
Dedication	viii
Acknowledgements	ix
1 Introduction	1
1.1 ATLAS Detector	3
1.2 Theory of Silicon Strip Detectors	3
1.3 Punch Through Effect and the PTP Structure	8
2 Measuring the punch-through effect	11
2.1 Laser injection apparatus	12
2.2 Calibration	12
2.3 Characterizing the PTP structure	17
3 Results	23
3.1 Voltage Measurements	23
3.2 PTP Resistance	25
4 Summary and Conclusion	31
5 Appendix	33
Bibliography	42

List of Figures

1.1	ATLAS Inner Detector with the semi-conductor tracker indicated by the two arrows. Courtesy of atlas.ch	4
1.2	Cross section of a generic P-on-N type silicon strip detector with an ionizing charged particle which creates electron/hole pairs. These electron/hole pairs are then swept away by the electric field which is created by reverse biasing the sensor. Courtesy of Hartmann.	5
1.3	Top view of the ATLAS 12 PZ1-P11 sensor. The BZ1 identifier characterizes the PTP geometry. During the sensor operation, a bias voltage is applied to the bias ring. The guard ring is designed to create a homogeneous electric field. AC coupled pads are connected to electronics and they transmit AC signal. When the particle interacts with the sensor, the amplifiers will see the resulting AC signal across the capacitance. The PTP structure and bias resistor is also indicated in the figure.	6
1.4	A 1-D illustration of the punch-through effect; a.) $V = 0$, b.) $0 < V < V_{pt}$, c.) $V = V_{pt}$, d.) $V > V_{pt}$. The locations of the depleted regions for each junction is given by x_0 and x_1 , with $x = 0$ and $x = 1$ being the locations of the junctions and E and V being the electric field and potential respectively.[1] Courtesy of Chris Betancourt et al.	9
2.1	Relative positions of laser near and far positions with respect to the PTP, bias, and implant resistors. The voltages V_{near} and V_{far} are measured with a oscilloscope. Courtesy of Chris Betancourt.	13
2.2	The PTP region on the ATLAS07 BZ3-P1 sensor. While testing, the bias ring is held to ground. PTP is the region between the end of the implant (reddish color) and the bias ring. The micropositioner probes are placed on the DC pads. The zigzagging trace is the bias resistor. The guard ring creates a homogeneous electric field inside the sensor. Finally, the laser is aimed in the vicinity of a DC pad.	13
2.3	Probing circuit diagram for laser injection testing using a IR cutting laser. The R1 and R2 resistors create a voltage divider.	14
2.4	G10 calibration pad used for calculating the attenuation factor. To test for noise introduced by the micropositioner probes, the pins on the G10 pad were directly connected to the DP amplifier.	16

2.5	Superimposed signals directly from pulser (ch 1), and the two differential probes (ch3 and 4). Note the different scales for the channels.	17
2.6	Arc damage in the form of a crater can be seen on the bias ring. The scratch to the left of the crater shows the size of the probe mark we use on bias ring. A mark can also be seen in the DC pad.	18
2.7	Readout voltage vs. time from the far probe on the ATLAS12 BZ3C-P16 sensor. Laser fired near. The oscilloscope was triggered on the noise at $t = 0$ and a variable time delay was set to only record the pulse which starts at $t \approx 125$	22
3.1	Far and near probe readout voltage vs. bias voltage for ATLAS12 BZ3C-P6 sensor. Laser fired far.	24
3.2	Far and near probe readout voltage vs. bias voltage for ATLAS12 BZ3C-P6 sensor. Laser fired near.	25
3.3	Near probe readout voltage pulse for ATLAS12 BZ3C-P6 sensor. Laser fired near. This is the first pulse after which the sensor's leakage current greatly increased.	26
3.4	Far and near probe readout voltage vs. bias voltage for ATLAS12 BZ3C-P16 sensor. Laser fired near.	27
3.5	$R_{PT(far)}$ on the ATLAS BZ3C P16 sensor vs. bias voltage. There is no correlation between $R_{PT(far)}$ and V_{bias} which indicates that the far punch through structure does not turn on.	28
3.6	$R_{PT(near)}$ on the ATLAS BZ3C P6 sensor vs. bias voltage. The resistance of near punch through structure is decreasing with increasing bias voltage which indicates that the structure is working and increasing the amount of charge sent to ground.	29
3.7	$R_{PT(near)}$ on the ATLAS BZ3C P6 sensor vs. V_{far}	30
3.8	$R_{PT(near)}$ on the ATLAS BZ3C P6 sensor vs. V_{near}	30
5.1	Value of R_{imp} is the inverse slope obtained from a linear fit (line) on current and voltage measurements (points).	37

List of Tables

2.1	R_{imp} values from ATLAS12 BZ3C P6 sensor.	20
2.2	R_{imp} values from ATLAS12 BZ3C P16 sensor.	20

To everybody

Acknowledgements

I acknowledge everyone at SCIPP. In particular, Vitaliy Fadeyev, Hartmut Sadrozinski, Zach Galloway, Matthew Domingo, Andriy Zatserklyaniy, and Marta Baselga. Last but not least, I would like to acknowledge my parents, Sergey and Alla Shumko who have supported me though my life and are the greatest parents I ever wished for.

1

Introduction

Our dependence on semi-conductors in technology is at an unprecedented level.

Semi-conductors are used in cell phones, CCD chips, computers, and assembly line robots, among a myriad of other uses. In physics, sensors composed of semi-conductors are utilized anywhere photons or charged particles need to be detected. In particle physics, semi-conductor technology "...provide[s] a unique combination of energy and position resolution." [2] These sensors allow particle colliders to accurately track the spatial coordinates of passing particles, and use this information to reconstruct intermediate particles and their interactions. Additionally, semi-conductors are indirectly used whenever measurements are analyzed with a computer.

As versatile these sensors are, they can malfunction and break when charged particles deposit more energy into their crystal lattice than they were designed. For particle colliders such as the Large Hadron Collider (LHC), the deposited energy can come from a misguided beam of protons. At the LHC, two proton beams, one rotating clockwise and the other counter-clockwise, are guided inside the 27 km circular tunnel by super-

conducting magnets which generate a 8.33 Tesla [3] magnetic field. The two beams of oppositely-orbiting protons are steered to intersect in four different caverns where the massive detectors are located. One of these caverns houses A Toroidal Large Hadron Collider Apparatus (ATLAS). The sensors examined in this research are prototypes for the ATLAS upgrade.

If the proton beam is mis-steered, it may hit the beampipe and collimators. This impact will generate a high flux of secondary particles from the interaction between all of the material. As a result, the detector would be showered by these secondary particles. Such accidents are called beam losses. A beam loss has not yet occurred at the LHC. Nevertheless, a beam loss could cause severe damage to the ATLAS detector which would take many years to rebuild. Since the amount of charge stored in the beam will increase after the LHC Upgrade, these sensors must be able to withstand a large amount of flux.

In the case of a beam loss, the flux larger than the sensors were designed for, they could experience damage or break. These damaged sensors would severely handicap the entire detector by reducing its acceptance. Replacing these sensors is costly and time consuming. To avoid permanently damaging the sensors from a fluence, or a large flux over a short period of time, the sensors must be equipped with a structure that re-routes the excess charge to ground. This structure is called the punch-through protection (PTP) which utilizes the punch-through effect. This thesis will explore the effectiveness of these structures that are components of the 2012 Generation ATLAS strip sensors.

The characterization of the PTP structure will help determine which types of punch-through structures are most effective at re-routing current to ground. This information can guide the sensor design during the follow-up refinement stages of development. In

addition, this information will help in protecting the sensitive readout electronics that are directly connected to the strip detectors.

1.1 ATLAS Detector

The predecessors of the ATLAS 2012 generation (ATLAS12) strip detectors are the ATLAS07 detectors. Both sensor models were developed by Hamamatsu Corporation. These strip detectors are made for sensor development for the upgrade. While these sensors will not be installed in ATLAS, they are similar to the sensors which make up the Semiconductor Tracker (SCT) in the inner detector of ATLAS, depicted in Fig 1.1. Santa Cruz Institute for Particle Physics (SCIPP), then headed by Abraham Seiden, had a major contribution to the inner detector development. Indicated in Fig. 1.1, overlapping tiles of these sensors surround the beam line. Due to its proximity to the beam line, the SCT will experience a large flux of secondary particles if the beam is mis-steered enough to hit the beampipe and collimators.

1.2 Theory of Silicon Strip Detectors

The simplest model for a silicon strip detector is a diode which is made of a positive and negative type silicon (P-type and N-type) that are directly connected. Silicon has four valence electrons. Thus, P-type silicon is made by adding elements which have less than four valence electrons to Silicon. This process is known as doping. The P-Type silicon has an excess of free, positively charged carriers which are called holes. A similar process is used to create N-type silicon, but the silicon is doped with an element with more than

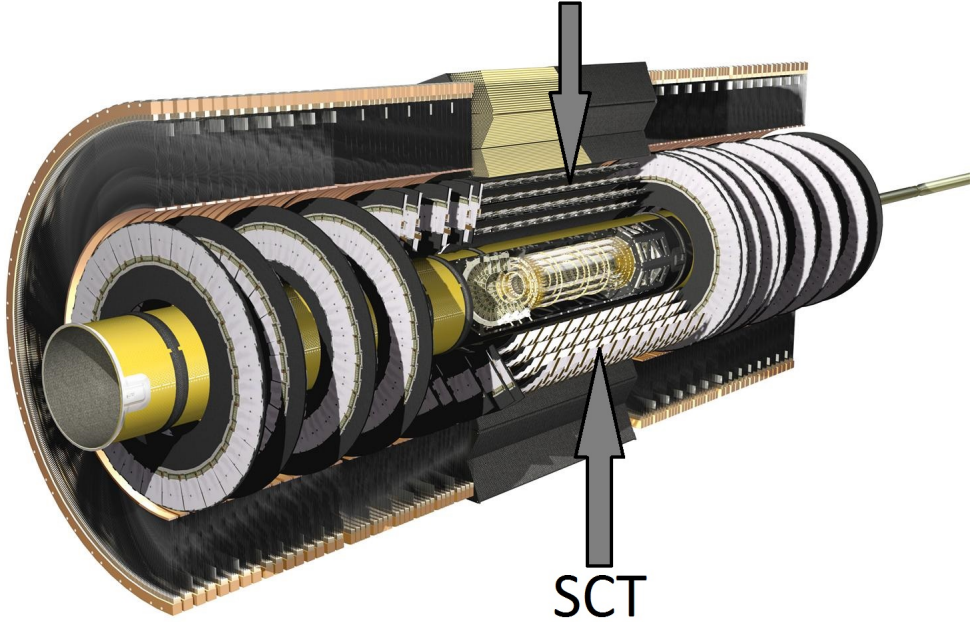


Figure 1.1: ATLAS Inner Detector with the semi-conductor tracker indicated by the two arrows. Courtesy of atlas.ch

four valence electrons. This doping creates free electron charge carriers. Intrinsic silicon is an insulator, but the free charges in doped silicon allows current to flow in a very useful manner. This is why silicon is known as a semi-conductor.

A P-N junction is a structure of N and P type Silicon joined together. In equilibrium, the N-type and P-type carriers diffuse into each other. The region in which charge carriers have diffused is called the depletion region¹ which is nearly absent of free charge carriers. The P-N junction is important because it is “...the fundamental building block of the electronic age” [5].

There are two types of silicon particle sensors, P-on-N and N-on-P. A cross-section

¹Hartman’s book[4] gives a more thorough discussion on the atomic properties of the p-n junction in diodes and silicon sensors.

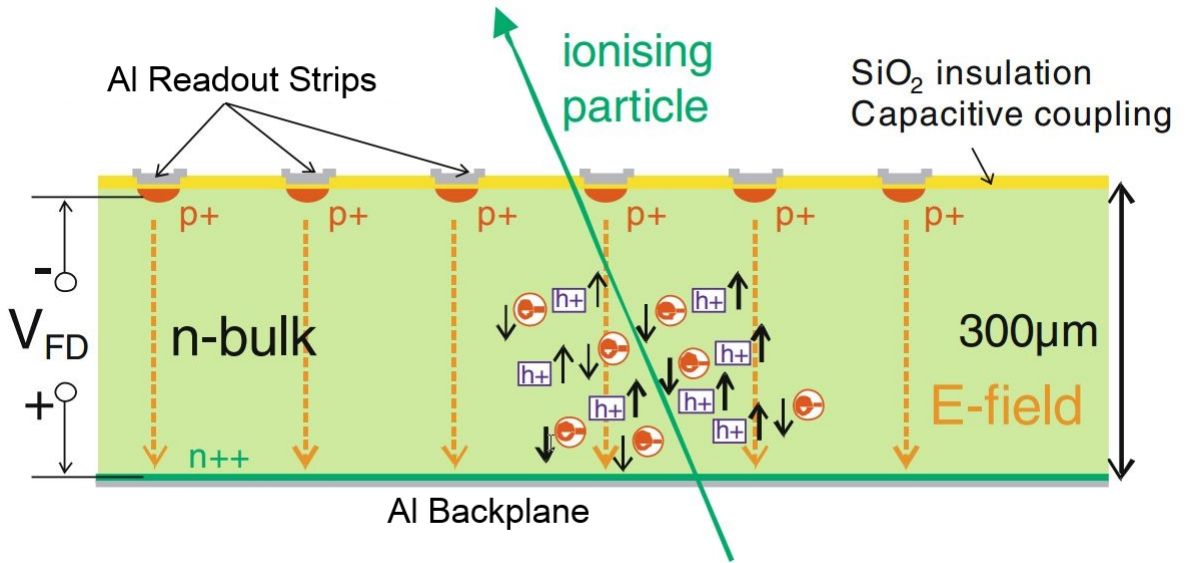


Figure 1.2: Cross section of a generic P-on-N type silicon strip detector with an ionizing charged particle which creates electron/hole pairs. These electron/hole pairs are then swept away by the electric field which is created by reverse biasing the sensor. Courtesy of Hartmann.

of a P-on-N sensor from top to bottom is given in Fig. 1.2. In a N-on-P sensor, the P and N type Silicon are switched. The aluminum strips and the aluminum backplane are similar to the two connectors in a capacitor. The sensors characterized in this thesis are N-on-P type sensors.

A N-on-P silicon sensor has two operating modes which are similar to that of a diode. In the forward bias operating mode, a bias voltage is applied to the aluminum backplane. The aluminum strip called the bias ring, which is shown in Fig. 1.3, is held at ground. Electrons will drift through the sensor toward the higher potential at the aluminum backplane. Conversely, holes drift toward the readout strips. As a result, current flows through the sensor.

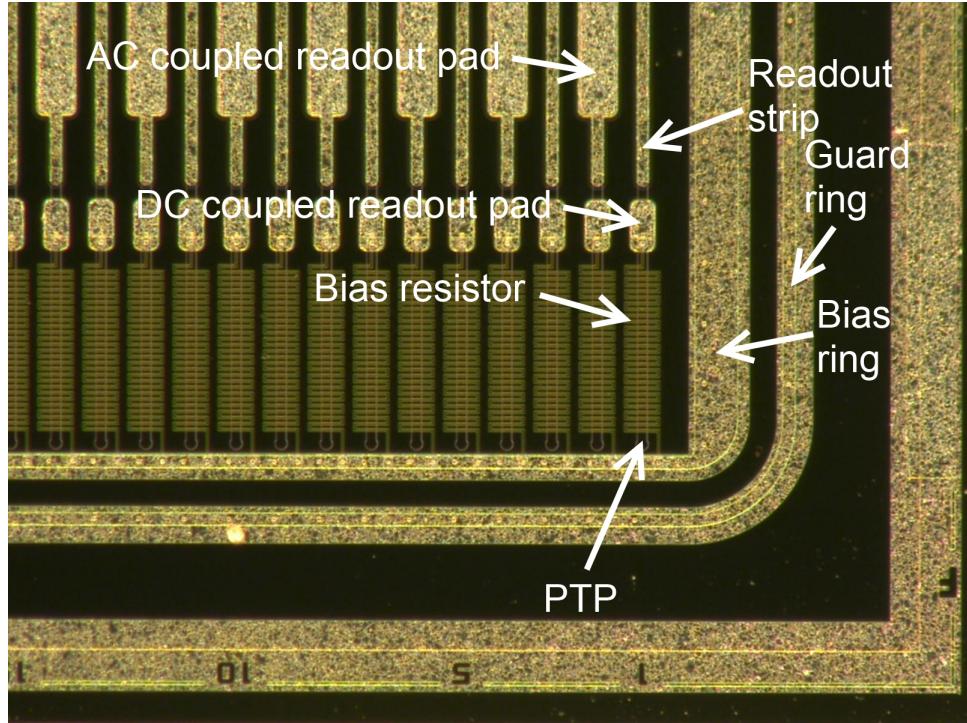


Figure 1.3: Top view of the ATLAS 12 PZ1-P11 sensor. The BZ1 identifier characterizes the PTP geometry. During the sensor operation, a bias voltage is applied to the bias ring. The guard ring is designed to create a homogeneous electric field. AC coupled pads are connected to electronics and they transmit AC signal. When the particle interacts with the sensor, the amplifiers will see the resulting AC signal across the capacitance. The PTP structure and bias resistor is also indicated in the figure.

On the contrary, in the reverse bias operating mode, a positive bias voltage is applied to the bias ring and the backplane is held at ground. In ideal circumstances, this circuit is identical to applying a negative potential to the backplane while keeping the bias ring at ground. In this mode, the electrons drift to the readout strips and the holes drift to the backplane. As a result, the Coulomb attraction between electrons and holes forms an electric field. This electric field forms a depletion region free of mobile charges and as a result, no current flows through the detector. This is the operating mode used for detecting particles.

When a charged particle passes through a biased sensor, the particle loses energy from the lattice interactions. For every 3.7 eV of energy transferred to the crystal lattice², an electron-hole pair is formed[2]. As shown in Fig. 1.2, these electron-hole pairs are swept apart by the electric field. The electrons migrate to the AC readout strips while holes migrate to the backplane. The AC pads are coupled by > 20 pF/cm[6] capacitor which operates up to 100 Volts[7]. The acquired charge on the readout strips is processed by electronics that analyze the signal.

A thicker depletion region will induce a larger signal. Thus, these sensors are operated at full depletion, at which the entire volume is depleted[4]. This is the minimal operational voltage for the sensor. The full depletion voltage[4], $V_{full\ depletion}$ is a function of the sensor thickness D , dialectic permittivity ϵ and sensor resistivity ρ is given by

$$V_{full\ depletion} = \frac{D^2}{2\epsilon\mu\rho}. \quad (1.1)$$

²While the discussion of calorimeters is beyond the scope of this thesis, the low ionization energy of silicon does not drastically alter the particle's energy so that the calorimeters can measure energy closer to its true value.

For ATLAS07 and ATLAS12 sensors, $V_{full\ depletion} = 170$ V and $D = 320$ Microns[6, 8]. The use of a single strip is extended to multiple, evenly-spaced strips. For the ATLAS07 and ATLAS12 sensors, the distance between strips, or pitch is $74.5\mu\text{m}$ [6, 8]. If the entire charge is collected on a single strip, the position resolution[1] is given by $\sigma = \text{pitch}/\sqrt{12}$. As a result, a more compact strip geometry increases the sensor's resolution in the dimension perpendicular to the strips.

1.3 Punch Through Effect and the PTP Structure

When too much charge is collected at a strip, the PTP structure must be utilized to avoid damaging the sensor. For simplicity, consider a one dimensional, N-P-N (or P-N-P) sandwich structure. By extending the mechanism presented in §1.2, two electric fields would exist at the junctions. Applying a voltage across the structure will forward bias one region and reverse bias the other. As seen in Fig. 1.4, as the applied voltage increases, the reverse biased electric field grows. At V_{pt} , or the punch-through voltage, the two electric fields touch. As a result, charge from the forward biased junction will be injected into the reversed bias junction, leading to an exponential rise in current with respect to applied voltage[1].

The PTP structure utilizes this effect which allows significant current to flow[1, 9, 10, 11] to ground once V_{pt} is reached. The structure is a region composed of the implant, the bulk, and the bias ring. As the potential difference between the implant and the bias ring reaches and surpasses V_{pt} , the PTP structure “turns on” and re-routes some of the current to the bias ring which is held at ground. These sensors are identified by the “BZ” (Baby Zone) naming convention, where the preceding number is between 1 and 6 and represents

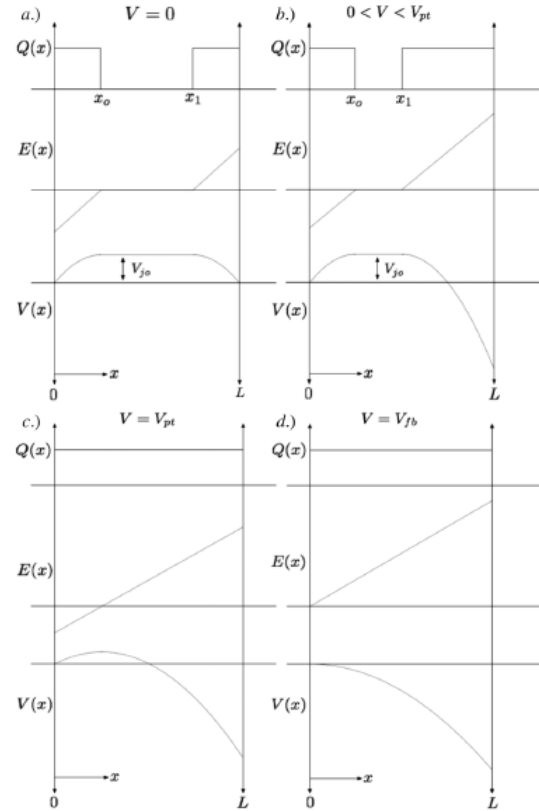


Figure 1.4: A 1-D illustration of the punch-through effect; a.) $V = 0$, b.) $0 < V < V_{pt}$, c.) $V = V_{pt}$, d.) $V > V_{pt}$. The locations of the depleted regions for each junction is given by x_0 and x_1 , with $x = 0$ and $x = 1$ being the locations of the junctions and E and V being the electric field and potential respectively.[1] Courtesy of Chris Betancourt et al.

the different PTP geometries.

2

Measuring the punch-through effect

A variety of techniques are employed to measure the punch-through effect in the PTP structure. The two methods which we used were DC and laser injection tests. The DC test is relatively simple to conduct and gives a good approximation of the PTP characteristics. A better approximation of the PTP characteristics can be obtained via laser injection. Laser injection tests are more complex to administer and are very sensitive. Nevertheless, they better mimic the dynamic effects of a beam loss since the laser is fired in short duration pulses.

In this study, ATLAS07 sensors were used to calibrate the laser testing setup and were compared the results to previous research. Then, the ATLAS12 prototype sensors were also tested using the setup. The sensor is biased using the bias ring indicated in Fig. 2.1, and the backplane. When biasing the sensor, it was important to keep the leakage current below a few Micro Amps and bias voltage below $-300V$. Nearly all sensors which were

biased to $-300V$ broke during testing. Also, note that a negative potential was applied to the backplane while the bias ring is held at ground. Because the oscilloscope probes were referenced to ground, the only way to bias the sensor was to apply a negative potential to the backplane.

2.1 Laser injection apparatus

We simulated beam losses with an Alessi LY1 IR laser which emits light at 1064 nm with a maximum power output of 10mJ over $70\mu s$ [12]. The laser was focused through a microscope onto the surface of the sensor. The laser beam was focused with a camera which outputted the microscope's view on a monitor. After the laser was fired at a metal surface, the resulting crater position was marked by an "X" on the monitor. This allowed us to have reliable positioning of the laser beam. The laser was operated at a power setting of "505", and was aimed in the vicinity of a DC pad near the bias resistor and on the opposite side. The convention "near" for the pads close to the bias resistor and "far" for the opposite side is adopted as seen in Fig. 2.1. Lastly, the laser was aimed at the silicon components between the strips to avoid potentially damaging the laser from a reflection. To avoid damaging the laser, the user manual states that the laser can be fired indefinitely at a rate of 3 seconds per pulse, or continuously for 30 seconds, with a 30 second cool down.

2.2 Calibration

To collect and measure charge from the sensor, the DC and AC pads shown in Fig. 2.1 were connected to a Tektronix P6246, 400 MHz Differential Probe (DP) and a

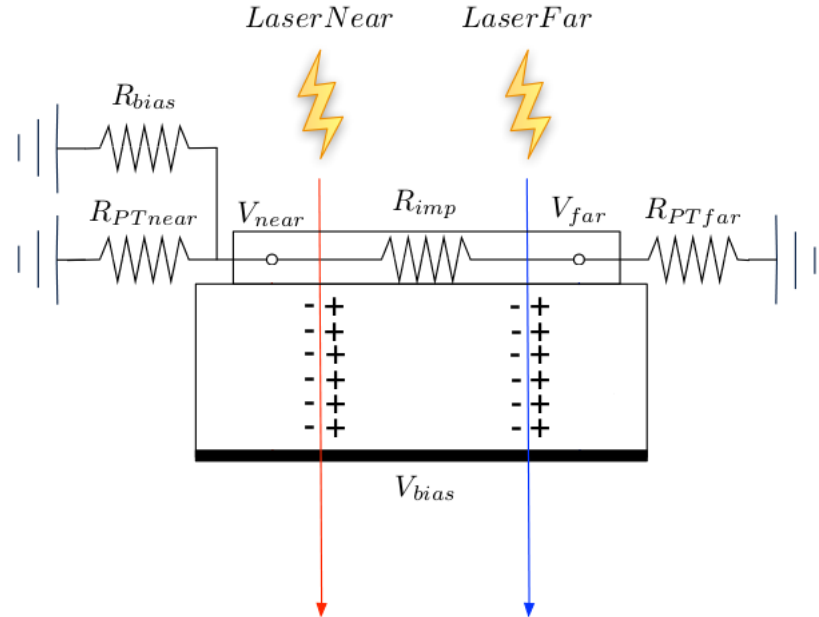


Figure 2.1: Relative positions of laser near and far positions with respect to the PTP, bias, and implant resistors. The voltages V_{near} and V_{far} are measured with an oscilloscope. Courtesy of Chris Betancourt.

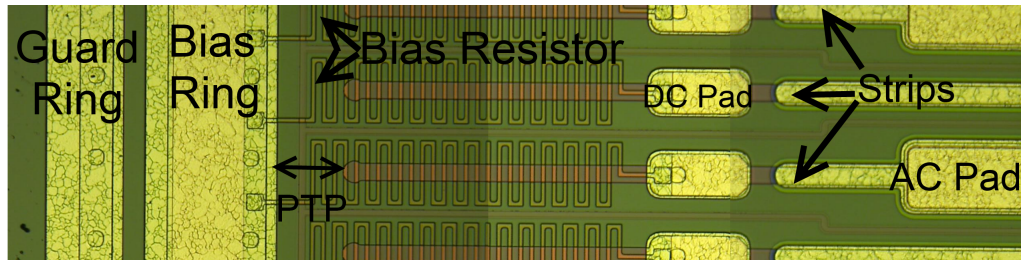


Figure 2.2: The PTP region on the ATLAS07 BZ3-P1 sensor. While testing, the bias ring is held to ground. PTP is the region between the end of the implant (reddish color) and the bias ring. The micropositioner probes are placed on the DC pads. The zigzagging trace is the bias resistor. The guard ring creates a homogeneous electric field inside the sensor. Finally, the laser is aimed in the vicinity of a DC pad.

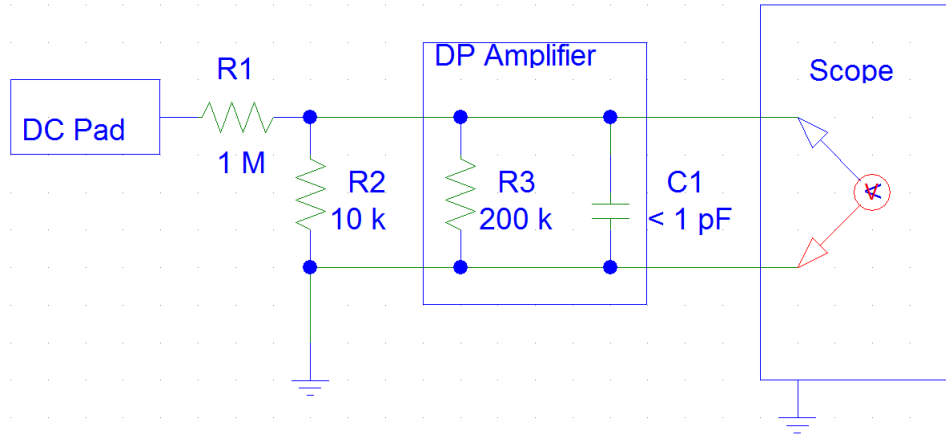


Figure 2.3: Probing circuit diagram for laser injection testing using a IR cutting laser. The R1 and R2 resistors create a voltage divider.

Tektronix P6247, 1 GHz DP which measure the potential difference between ground and the signal. The DPs were connected to a Tektronix TDS 5054 oscilloscope using the DP connector.

The differential probes are rated to a maximum voltage difference across the inputs of $\pm 850mV$ if the DP attenuation setting is set to 1, and $8.5V$ if the attenuation setting is set to 10. To avoid damaging the DPs, a voltage divider, which consists of resistors R1 and R2 depicted in Fig. 2.2 was integrated between the micropositioner probes and the differential probes. Because of stray inductance and capacitance, the probe setup attenuation factor was calibrated to determine its value at that time. The following steps were used to calculate the impedance of the circuit, from which the attenuation factor is subsequently calculated.

First, add R2 and R3 in parallel to find Z_{R2R3}

$$Z_{R2R3} = \frac{1}{\frac{1}{R2} + \frac{1}{R3}}$$

now add $R2\&3$ and $C1$ in parallel

$$Z_{RC} = \frac{Z_{R2R3}}{\sqrt{(2\pi \times \nu \times C \times Z_{R2R3})^2 + 1}}$$

where ν is the frequency and C is the capacitance of the capacitor shown in Fig. 2.2. Since a single pulse is measured, bandwidth is used instead of frequency. Bandwidth[13] is calculated by

$$\text{Bandwidth} = \frac{0.34}{\text{Rise time}_{10\% - 90\%}}$$

Finally, the voltage divider equation

$$\text{Attenuation} = \frac{V_{\text{in}}}{V_{\text{out}}} = \frac{R1 + Z_{RC}}{Z_{RC}}.$$

Using this result, the calculated theoretical attenuation factor was 106.

To find the actual attenuation factor of the circuit, the probe, voltage divider, and differential probes were calibrated using a pulse generator. A BNC cable connected the pulser to the oscilloscope, while the second cable was connected to a G10 copper pad shown in Fig. 2.4. A trench was machined in the middle of the G10 and both the core and ground of the BNC cable were connected to the two pads. A terminating 50Ω resistor was soldered between the two halves of the G10 to avoid ringing effects. Next, the two micropositioner probes were touched down on the core side of the G10. A pulse of a few volts was sent directly to the oscilloscope, and to the G10. Figure 2.5 shows the direct signal, and the signal from the differential probes were superimposed on the oscilloscope and their amplitudes measured. The ratios of the amplitudes of channel 1 (direct from

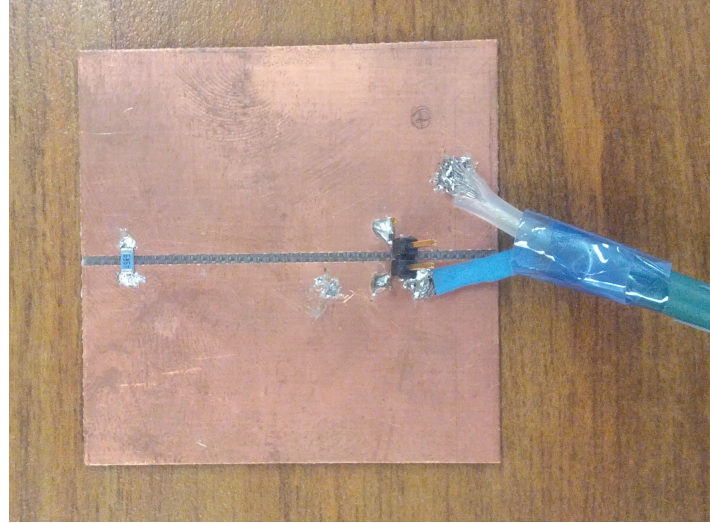


Figure 2.4: G10 calibration pad used for calculating the attenuation factor. To test for noise introduced by the micropositioner probes, the pins on the G10 pad were directly connected to the DP amplifier.

pulser) to channel 3 and channel 4 (differential probes) are the experimental attenuation factors which varied between 110 and 116.

The two probes have nearly identical attenuation factors. The individual attenuation factors were accounted for in the analysis by multiplying the signal by the attenuation. The range in attenuation factors can be caused by a variety of things including temperature stability of the oscilloscope and pulser, error in the value of the resistor, and precision of the oscilloscope's cursor function. We found similar attenuation factors obtained before and after 30 minutes of constant pulsing. Thus the calibration procedure may be done either before or after laser injection testing.

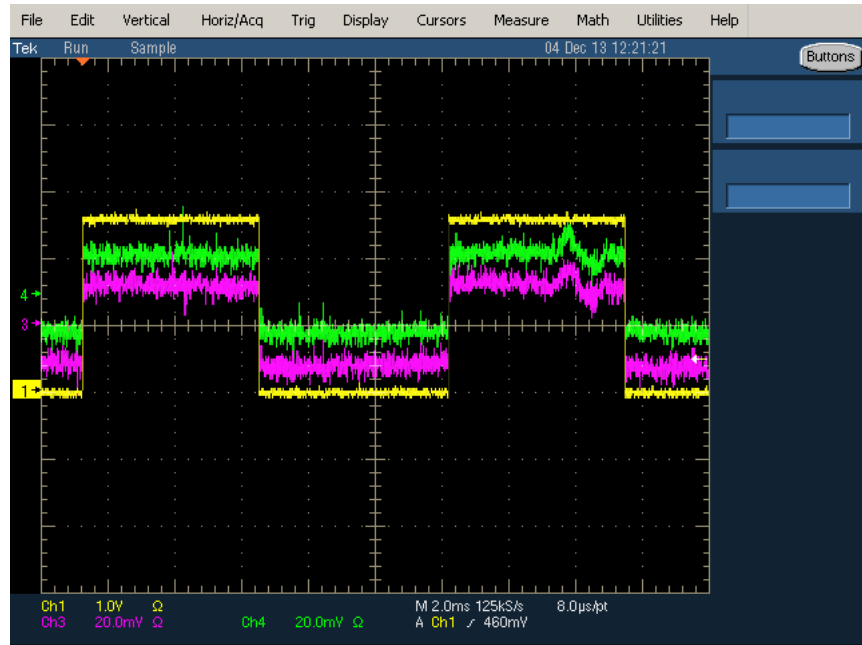


Figure 2.5: Superimposed signals directly from pulser (ch 1), and the two differential probes (ch3 and 4). Note the different scales for the channels.

2.3 Characterizing the PTP structure

In total, three probes were used for laser injection testing. One probe was connected to ground and was placed on the bias ring. In order to prevent damaging the sensor with an arc as in Fig. 2.6, a large skid mark was made to connect the bias ring to ground.

The two remaining probes were connected to the DPs and were placed on DC pads at either ends of the strip and their relative positions to the bias resistor were noted. The AC pads were not used to read out the voltage because earlier work[7] suggests that testing ATLAS07 sensors on AC coupled readout pads increases the likelihood of permanently damaging the sensor because the readout voltage may exceed the safe operating voltage of the coupling capacitor. ATLAS12 sensors have a similar coupling capacitor so only DC pads were read out.

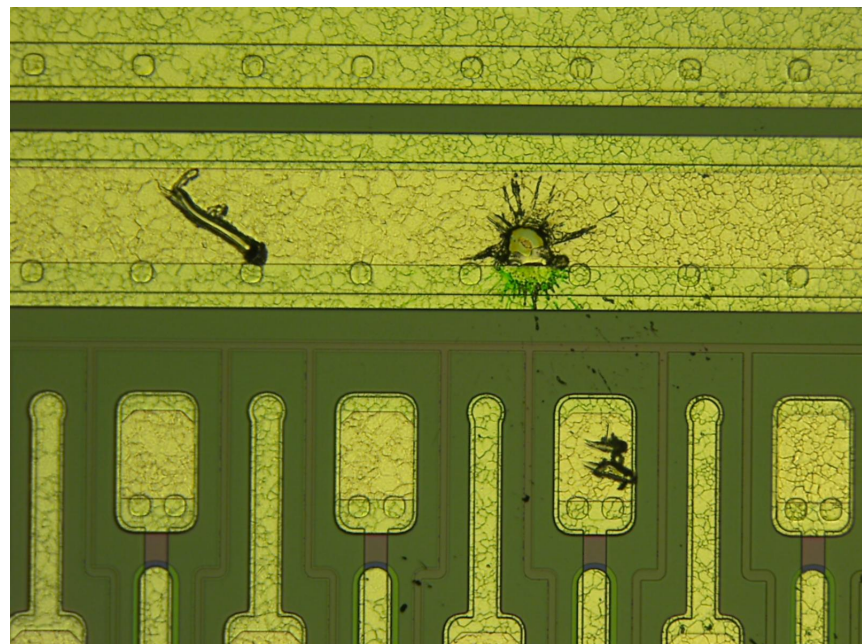


Figure 2.6: Arc damage in the form of a crater can be seen on the bias ring. The scratch to the left of the crater shows the size of the probe mark we use on bias ring. A mark can also be seen in the DC pad.

In this experiment, the laser aim and probe position remained constant, while the bias voltage was increased. Bias voltage step size was set at 25 V and ranged from 50 V to 250 V. Earlier studies tested the ATLAS07 sensors up to $V_{bias} = 300$ V[7, 14], but with this setup, all sensors laser tested at $V_{bias} = 300$ V developed a large and permanent leakage current. At each V_{bias} step, five pulses were recorded.

An example pulse is shown in Fig. 2.6. The observed noise at $t = 0$ was used to trigger the oscilloscope. The pulse relevant to the characterization of the PTP structure starts at around $t = 125 \mu s$ and has a very long tail.

From these pulses, the amplitude of the pulse was calculated with a C++ framework called ROOT. The baseline voltage, $V_{baseline}$ was calculated by averaging the first 100 points of each pulse. The peak amplitude, V_{peak} is ill-defined due to noise. A parabola was fitted in the region near the peak amplitude and the parabola's height parameter was used as V_{peak} . The pulse amplitude is the difference between the baseline and peak voltages, $V_{pulse} = V_{peak} - V_{baseline}$. The ROOT code for the program used to calculate the pulse amplitudes is included in Appendix A.

Conforming to the same convention as for the micropositioner probes, V_{near} corresponds to the pulse amplitude from near probe and V_{far} corresponds to the far probe. From Fig. 2.1, the final necessary measurement needed to calculate the PTP resistances is the implant resistance, R_{imp} . The testing procedure to calculate R_{imp} is given in Appendix B. Tables 2.1 and 2.2 show the measured values of R_{imp} for both ATLAS12 BZ3C P16 and ATLAS12 BZ3C P6 sensors. Both sensors have a similar R_{imp} in the range $14.77 - 14.94 \text{ k}\Omega$. With these measurements and the circuit diagram in Fig. 2.1, the PTP resistances, $R_{PT(near)}$ and $R_{PT(far)}$ are calculated.

Strip	V_{bias} (V)	R_{imp} ($k\Omega$)
20	-10	14.93
20	-50	14.94
20	-100	14.94
30	-10	14.93
30	-50	14.94
30	-100	14.94
40	-10	14.95
40	-50	14.96
40	-100	14.97
	AVERAGE	14.94

Table 2.1: R_{imp} values from ATLAS12
BZ3C P6 sensor.

Strip	V_{bias} (V)	R_{imp} ($k\Omega$)
20	-10	14.74
20	-50	14.74
20	-100	14.75
30	-10	14.78
30	-50	14.78
30	-100	14.79
40	-10	14.78
40	-50	14.78
40	-100	14.79
	AVERAGE	14.77

Table 2.2: R_{imp} values from ATLAS12
BZ3C P16 sensor.

Assume for both laser far and near that the ground is at $V = 0$ and V_{far} and V_{near} are referenced to ground. The two cases will be considered separately.

For laser injected near, it can be assumed that $V_{near} > V_{far}$. Then from the diagram in Fig. 2.1, the implant current, I_{imp} is given by

$$I_{imp} = \frac{V_{near} - V_{far}}{R_{imp}}$$

since the same current going through the implant is the same current going through $R_{PT(far)}$ and it is grounded,

$$R_{PT(far)} = \frac{V_{far} - V_{ground}}{I_{imp}} = \frac{V_{far} - 0}{I_{imp}} = \frac{V_{far}R_{imp}}{V_{near} - V_{far}} \quad (2.1)$$

On the contrary, for laser inject far, assume that $V_{far} > V_{near}$. Then the current in the implant is

$$I_{imp} = \frac{V_{far} - V_{near}}{R_{imp}}$$

which goes through both the R_{bias} and $R_{PT(near)}$ resistors which together is called R_{eff} .

Thus,

$$R_{eff} = \frac{V_{near} - V_{ground}}{I_{imp}} = \frac{V_{near} - 0}{I_{imp}} = \frac{V_{near}R_{imp}R_{bias}}{V_{far} - V_{near}}$$

where $R_{bias} = 1.5 \pm 0.5 M\Omega$ [8] and R_{eff} is given by

$$\frac{1}{R_{eff}} = \frac{1}{R_{bias}} + \frac{1}{R_{PT(near)}} \rightarrow \frac{1}{R_{PT(near)}} = \frac{1}{R_{eff}} - \frac{1}{R_{bias}}.$$

Now to put everything together,

$$\frac{1}{R_{PT(near)}} = \frac{V_{far} - V_{near}}{V_{near}R_{imp}} - \frac{1}{R_{bias}}$$

and simplify the expression,

$$R_{PT(near)} = \frac{V_{near}R_{imp}R_{bias}}{R_{bias}(V_{far} - V_{near}) - V_{near}R_{imp}} \quad (2.2)$$

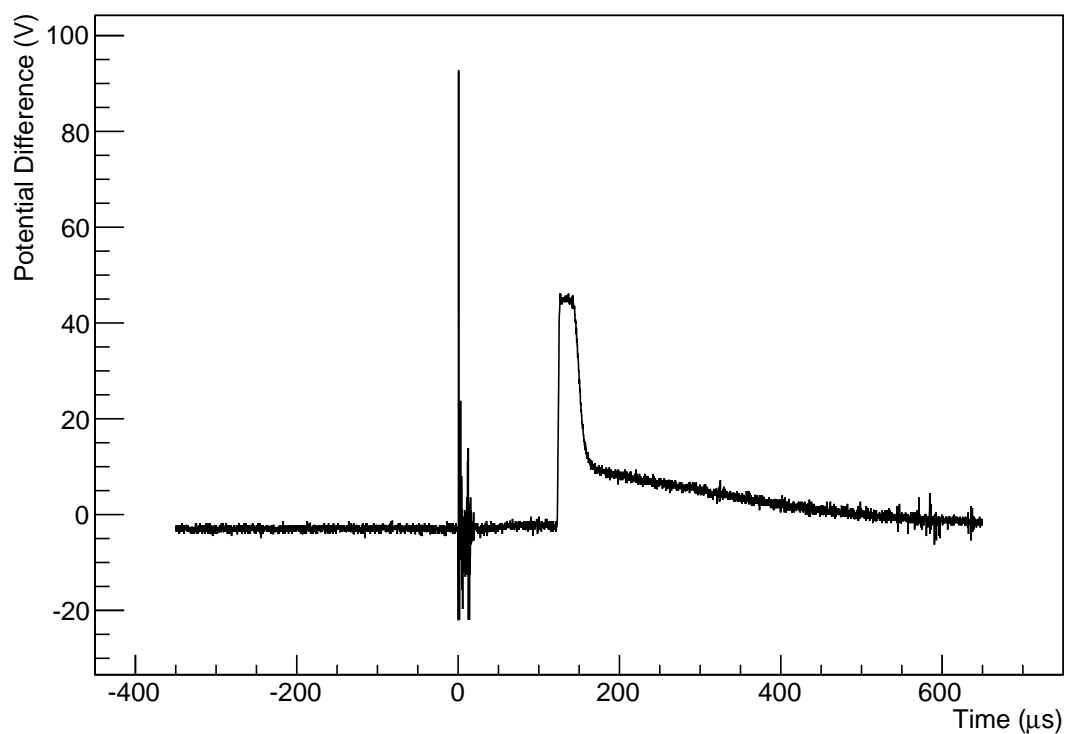


Figure 2.7: Readout voltage vs. time from the far probe on the ATLAS12 BZ3C-P16 sensor.

Laser fired near. The oscilloscope was triggered on the noise at $t = 0$ and a variable time delay was set to only record the pulse which starts at $t \approx 125$.

3

Results

3.1 Voltage Measurements

The readout voltage vs. bias voltage for the ATLAS12 BZ3C-P6 unpassivated sensor is shown for laser fired far (Fig. 3.1) and laser fired near (Fig. 3.2). A few comments regarding these results.

- The time scale of the width of ATLAS12 pulses are an order of magnitude greater than the width of the ATLAS07 pulses.
- Each voltage measurement shown in Figs. 3.1 and 3.2 is an average of five pulses.

The error bar is the standard deviation of the five pulses.

- The voltage measurements in Fig. 3.2 are incomplete because the sensor's leakage current increased by about an order of magnitude during laser testing at 125 V. V_{near} pulse shape at 125 V, shown in Fig. 3.3 exhibits an unusual shape when compared for Fig. 2.7.

- The large variance in Fig. 3.2 at $V_{bias} = 100$ V can be explained by the sensor beginning to malfunction.

- When the laser is fired far, V_{far} and V_{near} are very distinct while when laser is fired near, the voltage measurements are very similar. The reason is deduced from Fig. 2.1.

When laser is fired far, the current will follow the path of least resistance, that is, most current will flow to ground through $R_{PT(far)}$. On the contrary, when laser is fired near, $R_{eff} < R_{imp} + R_{PT(far)}$ and the current will flow directly to ground and little will go through the implant. The direct consequence is that $R_{PT(near)} < R_{PT(far)}$ which can be checked from Eqs. 2.1 and 2.2.

Figure 3.3 shows the V_{near} and V_{far} vs. V_{bias} for the ATLAS12 BZ3C-P16 sensor.

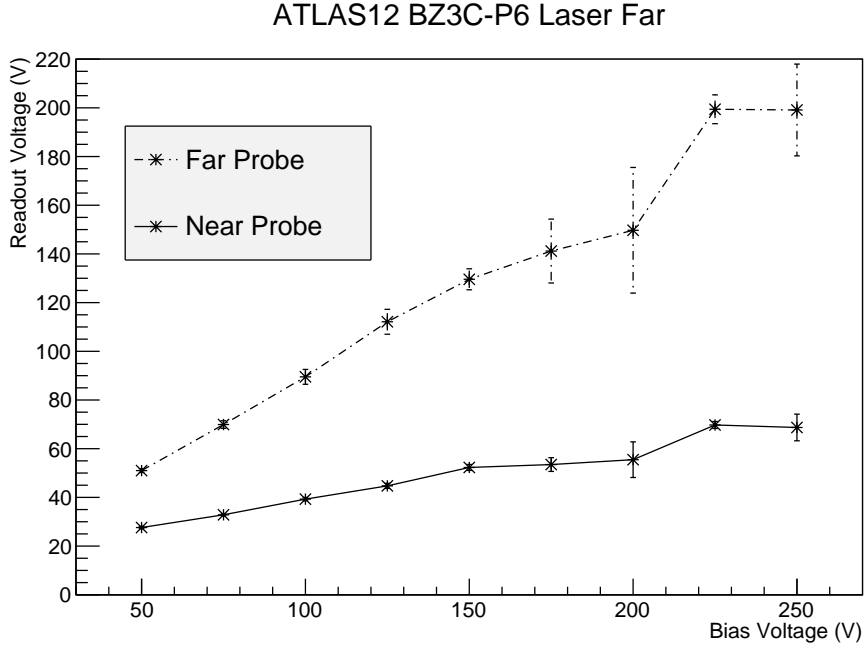


Figure 3.1: Far and near probe readout voltage vs. bias voltage for ATLAS12 BZ3C-P6 sensor. Laser fired far.

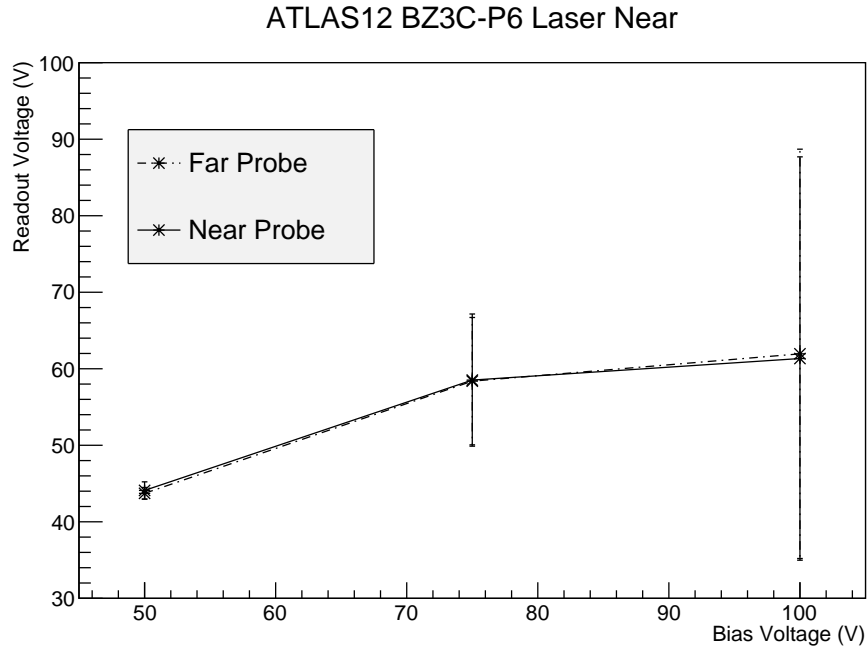


Figure 3.2: Far and near probe readout voltage vs. bias voltage for ATLAS12 BZ3C-P6 sensor. Laser fired near.

3.2 PTP Resistance

Using Eqs. 2.1 and 2.2, and a ROOT program in Appendix C, the resistances of the near and far PTP structures on ATLAS12 BZ3C-P16 sensors were calculated. Figure 3.4 shows $R_{PTP(far)}$ as a function of V_{bias} . The values are very scattered and there is no general trend to indicate that the PTP structure has activated. The denominator in Eq. 2.1 is the difference of V_{near} and V_{far} and from Fig. 3.2, the difference is very small. As the difference shrinks, $R_{PTP(far)}$ will become less well measured. Thus these measurements are very strongly influenced by systematic errors in the readout electronics and the fitting program shown in Appendix B.

Figure 3.5 shows a non-linear correlation of $R_{PTP(near)}$ as a function of V_{bias} .

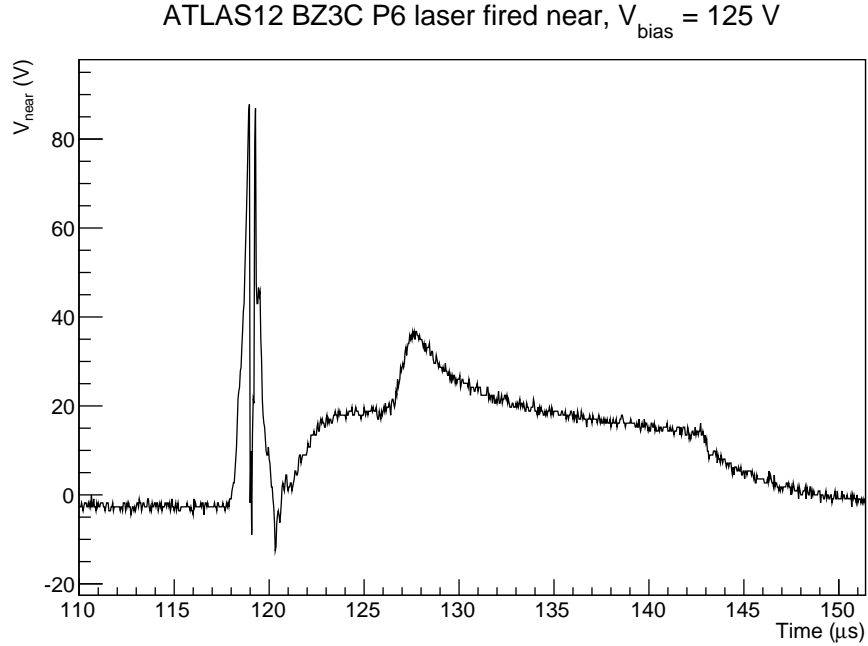


Figure 3.3: Near probe readout voltage pulse for ATLAS12 BZ3C-P6 sensor. Laser fired near. This is the first pulse after which the sensor's leakage current greatly increased.

$R_{PT(near)}$ decreases with increasing bias voltage which indicates that the PTP structure activated. These results are similar to the results obtained from the ATLAS07 devices[7]. Figures 3.6 and 3.7 show $R_{PT(near)}$ as a function of V_{far} and V_{near} , respectively. $R_{PT(near)}$ is decreasing as a function of the near and far probe peak voltages.

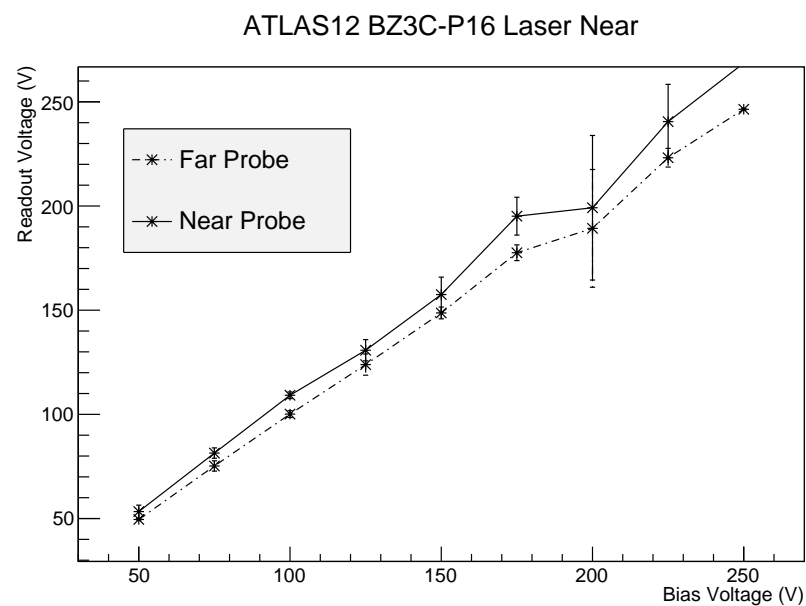


Figure 3.4: Far and near probe readout voltage vs. bias voltage for ATLAS12 BZ3C-P16 sensor. Laser fired near.

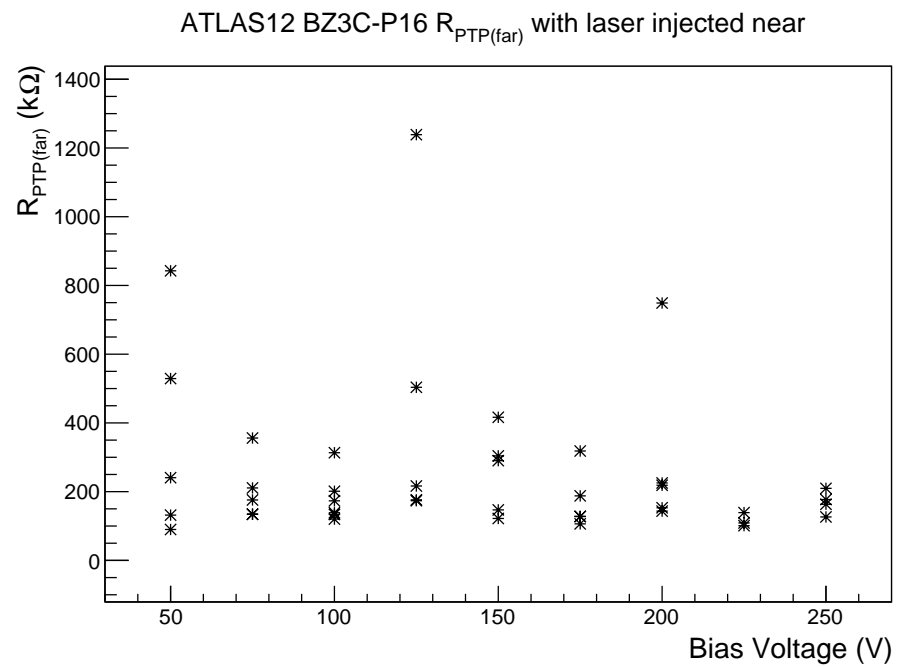


Figure 3.5: $R_{\text{PT(far)}}$ on the ATLAS BZ3C P16 sensor vs. bias voltage. There is no correlation between $R_{\text{PT(far)}}$ and V_{bias} which indicates that the far punch through structure does not turn on.

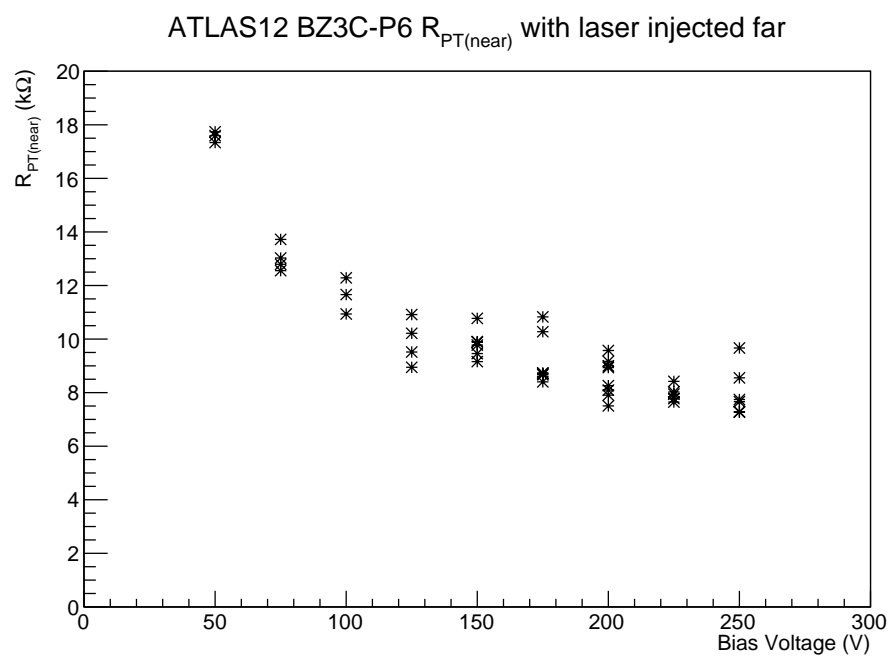


Figure 3.6: $R_{PT(near)}$ on the ATLAS BZ3C P6 sensor vs. bias voltage. The resistance of near punch through structure is decreasing with increasing bias voltage which indicates that the structure is working and increasing the amount of charge sent to ground.

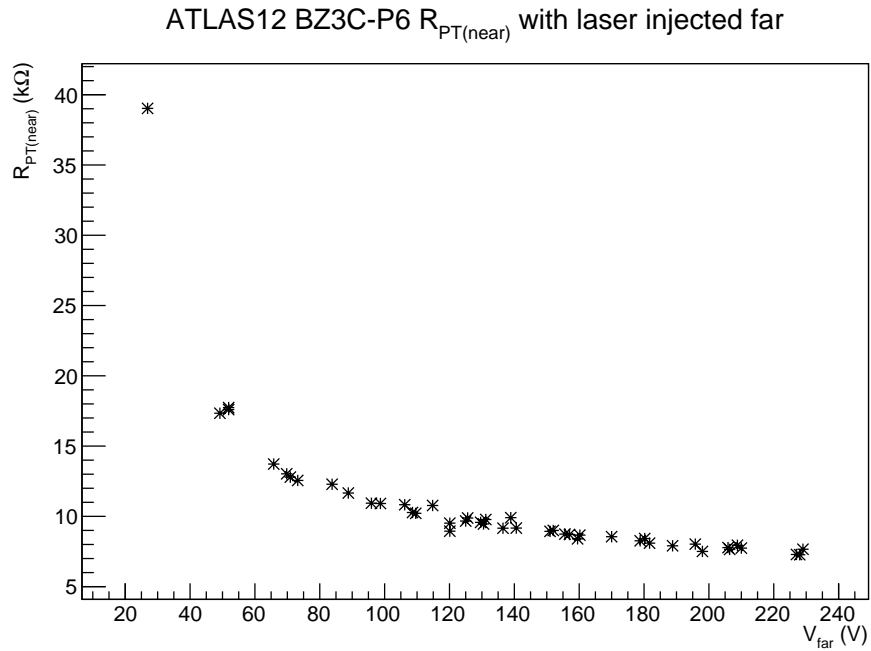


Figure 3.7: $R_{PT(near)}$ on the ATLAS BZ3C P6 sensor vs. V_{far} .

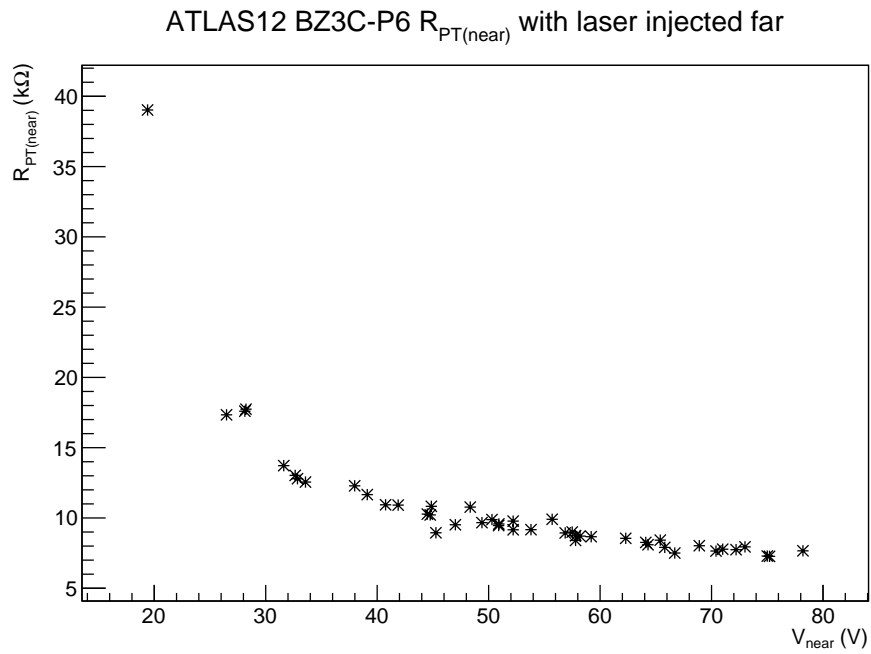


Figure 3.8: $R_{PT(near)}$ on the ATLAS BZ3C P6 sensor vs. V_{near} .

4

Summary and Conclusion

Large implant voltages, caused by laser testing or beam losses have the potential to damage silicon sensors. If the capacitors that connect the implant to the readout electronics are damaged, those channels would become useless. As was seen from the ATLAS12 BZ3C P6 sensor, the leakage current greatly increases as a result of the damage. This will prevent the sensor from properly functioning at the full depletion voltage, at which the sensor is the most sensitive to charged particles. A more moderate laser injection of charge shows that the near PTP structure on ATLAS12 BZ3C P6 activated and $R_{PTP(near)}$ decreased from roughly $18 \text{ k}\Omega$ at $V_{bias} = 50 \text{ V}$ to $9 \text{ k}\Omega$ at $V_{bias} = 250 \text{ V}$. The far PTP structure on ATLAS12 BZ3C P16 has a resistance which is roughly $200 \text{ k}\Omega$ and it does not have any correlation between $R_{PTP(far)}$ and V_{bias} . The calculations used to calculate $R_{PTP(far)}$ are very sensitive to V_{near} and V_{far} voltage measurements which diverge the closer the two voltages are. A more shielded and accurate testing setup with a more stable laser system is more suitable to calculate $R_{PTP(far)}$.

With this laser injection setup, $R_{PTP(near)}$ can be well measured for the other PTP

geometries on the ALTAS12 sensors. It will be then possible to determine the most effective PTP geometry. A more effective PTP structure is characterized by a lower resistance and will greatly minimize the damage from a beam loss at the LHC.

5

Appendix

A. ROOT code to calculate peak amplitudes and plot pulses

```
*****
* Name: pulse_amplitude.c
*
* Use: Calculates the pulse amplitude using a
* parabolic fit. Program also plots the pulse for
* visual inspection. Pass full path and file name
* into argument of fmain().
*
* Dependencies: tek.C
*
* File Format: The tektonic data output without
* commas.
*
* Output: Plot of the pulse. Uses a parabolic fit
* around the absolute peak to average out the
* noise and calculate the maximum amplitude.
*
* Written by Mykhaylo Shumko
*****
```

```
#include <iostream.h>
#include "TGraph.h"
#include "TF1.h"
#include "TLatex.h"
using namespace std;
```

```

int fmain(const char* ifname)
{
int i, j, k;
void readtek();
//const char* ifname = "far_300vBias_000.txt";
Int_t const np = 5000;
Double_t x[np], y[np];

Double_t flatV = 0;
Double_t attinuation = 112;
Double_t maxV = -1; // Maximum Amplitude (V)
Double_t maxInd; //Indicie value at the maxV
Double_t prePulse[np], pulsePeak[np]; //, pulsePeakAvg[np];

readtek(np, x, y, ifname);
for (i = 0; i < np; i++)
{
x[i] *= 1000000;
y[i] *= -attinuation; // Make the pulse
voltage positive & multiple by attinuation.
}
for (j = 0; j < 100; j++) flatV += y[j];
//Add first 100 points.
flatV /= 100;
// Divide the sum by 100 to get the ground voltage.

// Find maximum amplitude and indicie at maximum
amplitude.
for (j = 0; j < np; j++)
{
if(maxV < y[j])
{
maxV = y[j];
maxInd = j;
}
}

for (int i = 0; i < np; i++)
{
prePulse[i] = flatV;
pulsePeak[i] = maxV;
//pulsePeakAvg[i] = pulseMaxAverage;
}

printf("%f %f %f \n", flatV, maxInd, maxV);

```

```

TGraph *gr = new TGraph(np, x, y);
//TGraph *gr2 = new TGraph(np, x, prePulse);
//TGraph *gr3 = new TGraph(np, x, pulsePeak);
//TGraph *gr4 = new TGraph(np, x, pulsePeakAvg);

gr->GetXaxis()->SetTitle("Time (#mus)");
gr->GetYaxis()->SetTitle("V_{near} (V)");
gr->SetTitle("ATLAS12 BZ3C P6 laser fired
near, V_{bias} = 125 V");
gr->SetMarkerStyle(20);
gr->SetMarkerColor(4);
//gr2->SetLineColor(4);
//gr2->SetLineWidth(3);
//gr3->SetLineColor(4);
//gr3->SetLineWidth(2);

new TCanvas();
gr->Draw("AL");
TAxis *axis = gr->GetXaxis();
//axis->SetLimits(0.0001,.0002);
// axis->SetLimits(110,500);
//gr2->Draw("CP");
// gr3->Draw("CP");

TF1* parabolaFit = new TF1("Parabola", "[0] - [1]*(x-[2])*(x-[2])",
x[maxInd] - 0.5, x[maxInd] + 0.5); // .1244 to .1251
parabolaFit->SetParameters(maxV, 1.18547e12, x[maxInd]);
gr->Fit(parabolaFit, "R", "", x[maxInd] - 0.5, x[maxInd] + 0.5);

Double_t fitMaxA = parabolaFit->GetParameter(0);

printf("Pulse amplitude with fit is: %f \n", (fitMaxA - flatV));
printf("Pulse amplitude using global extrema: %f \n", (maxV - flatV));

return 0;
}

```

B. Implant resistance measurement

To measure the implant resistance R_{imp} , three micropositioner probes are used.

One is used to ground the bias ring. The two other probes touch down on the near and

far DC pads. The near probe and the bias probe are shorted so the near DC pad is also at ground. Analytically, R_{imp} is calculated by

$$R_{imp} = \frac{V_{far} - V_{near}}{I_{imp}}$$

where the voltage on the near DC pad, $V_{near} = 0$ if the near probe and bias probe are shorted. A voltage is applied to the backplane to bias the sensor. A small voltage starting at 0 V is then applied to the far probe and the voltage is increased in 0.1 V steps until 5 V is reached. Meanwhile, the current is measured from the far probe. With the voltage range and step size, 51 voltage and current measurements will be made which is enough to determine the linearity of the current with respect to applied voltage.

With these measurements, the differential resistance is calculated by

$$R_{imp} = \frac{\Delta(V_{far} - V_{near})}{\Delta(I_{imp})}$$

which is just the slope of a voltage vs. current plot. Figure 5.1 shows the measurements with a linear fit. The ROOT code used to generate the plot and calculate R_{imp} is given below.

Once R_{imp} is measured at a specific bias voltage and strip, it is useful to test the resistance at a different bias voltage to determine if a correlation between V_{bias} and R_{imp} exists. In addition, it is useful to test multiple strips to test if some strips have different resistances.

```
*****
* Name: IImplantResistance.c
*
* Use: calculates the differential implant resistor
* value from a linear fit on voltage and current in
* data file "f".
*
```

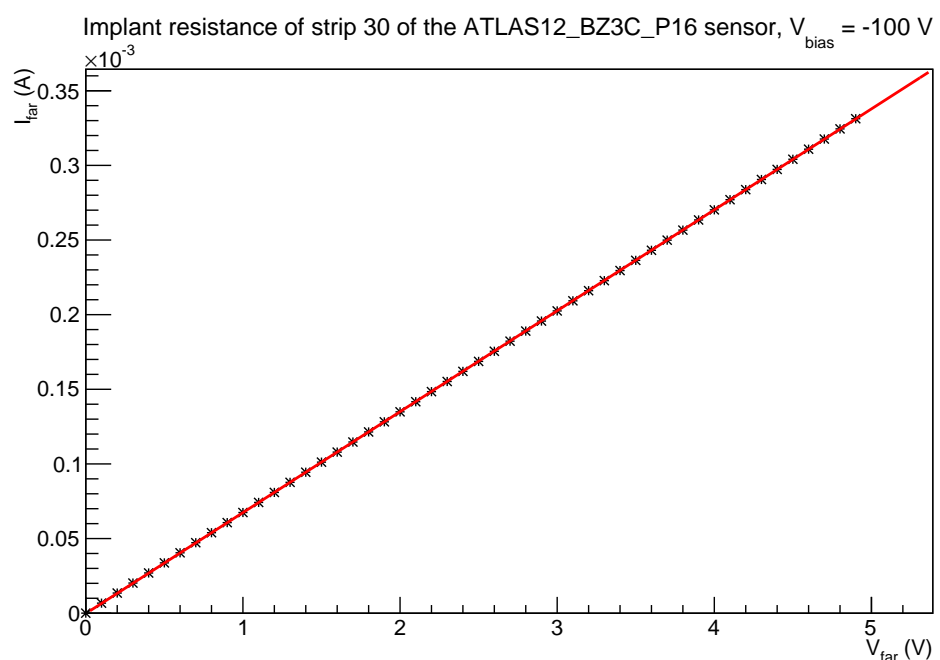


Figure 5.1: Value of R_{imp} is the inverse slope obtained from a linear fit (line) on current and voltage measurements (points).

```

* File Format: measurement number, bias voltage,
* bias current, far voltage, far current, near voltage,
* near current.
*
* Output: The differential resistance value obtained
* from the slope of the linear fit. Also plots the
* data and superimposes the linear fit.
*
* Written by Mykhaylo Shumko
***** */

#include <iostream.h>
#include "TGraph.h"
#include "TF1.h"
#include "TLegend.h"
#include "TLatex.h"
using namespace std;

int fmain()
{
    FILE * f;
    f = fopen("ATLAS12_BZ3C_P16_-100VBias_strip_30.TXT", "r"); // Open file.
    if (!f) // Stop if file is not found.
    {
        printf("Could not open file. \n");
        return 0;
    }

    const Int_t N = 50; Number of lines of data.
    Int_t i = 0;
    double no[N], biasV[N], biasI[N], farV[N], farI[N], nearV[N], nearI[N];

    while(i < N) // Read in file.
    {
        fscanf(f, "%lf %lf %lf %lf %lf %lf", &no[i],
               &biasV[i], &biasI[i], &farV[i], &farI[i], &nearV[i], &nearI[i]);
        i++;
    }
    fclose(f);

    // Plotting commands
    TGraph *farProbe = new TGraph(N, farV, farI);
    new TCanvas();
    TAxis *xaxis = farProbe->GetXaxis();
    TAxis *yaxis = farProbe->GetYaxis();
    farProbe->SetTitle("Implant resistance of strip")

```

```

30 of the ATLAS12_BZ3C_P16 sensor, V_{bias} = -100 V");
xaxis->SetTitle("V_{far} (V)");
yaxis->SetTitle("I_{far} (A)");
farProbe->SetLineStyle(5);
farProbe->Draw("AL*");

// Fitting
TF1* linFit = new TF1("Linear fit", "[0] + [1]*x",
farV[0], farV[N]); // Create fit object which exists
in the same range as the voltage.
linFit->SetParameters(0, 6.76954e-05); // Give initial guesses.
farProbe->Fit(linFit, "Q");
Double_t conductivity = linFit->GetParameter(1);
printf("Implant resistance is %e \n", 1/conductivity);
return 0;
}
return 0;
}

```

C. ROOT code to calculate $R_{PT(near)}$ and $R_{PT(far)}$

```

*****
* Name: ptp_resistance.c
*
* Use: Calculates the near and far PTP resistance.
*
* File Format: Data in the format: bias voltage,
* far voltage, bias voltage, near voltage.
*
* Output: Plot of the pulse. Uses a parabolic fit
* around the absolute peak to average out the
* noise and calculate the maximum amplitude.
*
* Written by Mykhaylo Shumko
*****/

#include <iostream.h>
#include "TGraph.h"
#include "TF1.h"
#include "TLegend.h"
#include "TLatex.h"
using namespace std;

```

```

int fmain()
{
Double_t Rimp = 14.7E3; //Ohms
Double_t Rbias = 1.5E6; //Ohms
const Int_t N = 46; // Number of lines in data file "f".
Int_t i = 0;
double biasV[N], farV[N], nearV[N], rFar[N], rNear[N];

FILE * f;
f = fopen("ATLAS12_BZ3C_P16_laser_near.txt" , "r"); // Open file "f".
if (!f)
{
printf("Could not open file. \n");
return 0;
}

while(i < N) // Read file "f".
{
fscanf(f, "%lf %lf %lf %lf", &biasV[i], &farV[i], &biasV[i], &nearV[i]);
i++;
}
fclose(f);

// Calculate PTP resistances.
for (i = 0; i < N; i++)
{
if (nearV[i] != farV[i]) //Avoid dividing by 0.
{
rFar[i] = Rimp*farV[i]/(nearV[i] - farV[i])/1000; // Far PTP calculation
printf("%.3d %10.4f %f %E\n", biasV[i], farV[i], nearV[i], rFar[i]);
}
rNear[i] = Rbias*Rimp*nearV[i]/(Rbias*(farV[i] - nearV[i]) - Rimp*nearV[i])/1000;
// Near PTP calculation
printf("%.3d %10.4f %f %E\n", biasV[i], farV[i], nearV[i], rNear[i]);
}
///////////
// Plot results.
TGraph *nearPTPR = new TGraph(N, biasV, rFar);
// If laser fired far, last argument of TGraph is "rFar". If laser fired near,
// last argument of Tgraph is "rNear"
TAxis *xaxis = nearPTPR->GetXaxis();
TAxis *yaxis = nearPTPR->GetYaxis();
nearPTPR->SetTitle("ATLAS12 BZ3C-P16 R_{PTP(far)} with laser injected near ");
//xaxis->SetLimits(0, 300);
//yaxis->SetRangeUser(0, 20);

```

```
xaxis->SetTitleSize(0.045);
yaxis->SetTitleSize(0.045);

xaxis->SetTitle("Bias Voltage (V)");
yaxis->SetTitle("R_{PTP(far)} (k#Omega)");

new TCanvas();
nearPTPR->SetLineStyle(5);
nearPTPR->Draw("A*");

return 0;
}
```

Bibliography

- [1] Chris Betancourt et al. The punch-through effect in silicon strip detectors. *IEEE Transactions on Nuclear Science*, 59(3):671 – 684, June 2012.
- [2] Juerg Beringer et al. *Particle Physics Booklet*. Physical Review, 2012.
- [3] European Organization for Nuclear Research. CERN FAQ LHC the guide, 2009.
- [4] Frank Hartmann. *Evolution of Silicon Sensor Technology in Particle Physics*, volume 231. Springer, 2009.
- [5] Alistair Sproul. Understanding the p-n junction.
- [6] Supply of Silicon Microstrip Sensors of ATLAS07 specification, October 2007.
- [7] Colin Parker. Tolerance to large injected charges in silicon strip detectors. Master's thesis, University of California Santa Cruz, June 2012.
- [8] Supply of Silicon Microstrip Sensors of ATLAS12 specification, May 2012.
- [9] S. Sze et al. Current transport in metal-semi-conductor-metal (MSM) structures. *Solid-State Electron*, 14:1209–1218, 1971.

- [10] J. Chu et al. Thermionic injection and space-charge-limited current in reach-through p+np+ structures. *Journal of Applied Physics*, 43:3510–3515, 1972.
- [11] J. Lohstroh et al. Punch-through currents in p+np+ and n+np+ sandwich structures. *Solid-State Electron*, 24:805, 1981.
- [12] Alessi Inc. LY1 Laser Cutting System User Manual.
- [13] Rise Time. http://en.wikipedia.org/wiki/rise_time.
- [14] Chris Betancourt. The punch-through effect in silicon strip detectors. Master's thesis, University of California Santa Cruz, June 2011.